Title	A theoretical study of cyclic ether formation reactions
Author(s)	Bugler, John; Power, Jennifer; Curran, Henry J.
Publication Date	2016-06-09
Publication Information	Bugler, John, Power, Jennifer, & Curran, Henry J. (2017). A theoretical study of cyclic ether formation reactions. Proceedings of the Combustion Institute, 36(1), 161-167. doi: https://doi.org/10.1016/j.proci.2016.05.006
Publisher	Elsevier
Link to publisher's version	https://doi.org/10.1016/j.proci.2016.05.006
Item record	http://hdl.handle.net/10379/6649
DOI	http://dx.doi.org/10.1016/j.proci.2016.05.006

Title Page

A Theoretical Study of Cyclic Ether Formation Reactions

John Bugler[a,*], Jennifer Power[a], Henry J. Curran[a]

[a]Combustion Chemistry Centre, National University of Ireland, Galway, Ireland

Corresponding author:

John Bugler,

School of Chemistry,

National University of Ireland, Galway,

Ireland.

Email: j.bugler1@nuigalway.ie

Colloquium: REACTION KINETICS

1

A Theoretical Study of Cyclic Ether Formation Reactions

John Bugler[a,*], Jennifer Power[a], Henry J. Curran[a]

[a]Combustion Chemistry Centre, National University of Ireland, Galway, Ireland

Abstract

Cyclisation reactions of hydroperoxyl-alkyl radicals forming cyclic ethers and hydroxyl radicals play an important role in low temperature oxidation chemistry. These reactions contribute to the competition between radical chain propagation and chain branching reaction pathways which dominate the reactivity of alkanes at temperatures where negative temperature coefficient (NTC) behaviour is often observed. The current study presents quantum chemically derived high-pressure limit rate coefficients for all cyclisation reactions leading to cyclic ether formation in alkanes ranging in size from C_2 to C_5. Ro-vibrational properties of each stationary point were determined at the M06-2X/6-311++G(d,p) level of theory. Coupled cluster (CCSD(T)) and Møller-Plesset perturbation theory (MP2) methods were employed with various basis sets and complete basis set extrapolation techniques to compute the energies of the resulting geometries. These methods, combined with canonical transition state theory, have been used to determine 43 rate coefficients, with enough structural diversity within the reactions to allow for their application to larger species for which the use of the levels of theory employed herein would be computationally expensive. The validity of an alternative, and computationally less expensive, technique to approximate the complete basis set limit energies is also discussed, together with implications of this work for combustion modelling.

1. Introduction

In recent years, there has been a proliferation of systematic theoretical studies concerning reaction pathways of importance in the low-temperature oxidation of alkanes [1–8]. The rapid increase in the number of studies of this kind is due, in part, to more readily available computational resources. This, coupled with the computationally inexpensive yet relatively accurate compound methods [9–15], as implemented in the Gaussian software packages [16], has aided the investigation of large arrays of reactions for which little or no experimental data are currently available. Several studies have determined high-pressure limit rate coefficients for large numbers of reactions within the important low-temperature reaction classes. Significant success has been achieved in chemical kinetic modelling of alkane oxidation systems by utilising these values [17–19]. Despite these successes, it has been highlighted that refinement of some important kinetic parameters is still necessary for further progress [17]. Particular disparity is seen amongst literature values for the title reactions. As is the case with many of the important uni-molecular reactions within the low-temperature oxidation pathways, most theoretical rate coefficients for the reactions of interest in this study have previously been derived using the CBS-QB3 compound method [9]. This is a popular method, particularly when studying large quantities of species and/or reactions, due to its relative speed and reliability [20]. Although relatively cost-effective, it has previously been highlighted as being potentially biased towards the under-prediction of reaction barrier in some instances [21]. For the reaction class of interest in this work, there may also be evidence of this based on investigations by Villano *et al*. [7], where an average difference of approximately 2.4 kcal mol^{-1} in 0 K barriers is observed between their values and those of DeSain *et al*. [22]. The barriers calculated by Villano *et al*. using the CBS-QB3 method are consistently lower than those calculated for the same reactions by DeSain *et al*., who used a combination of quadratic configuration interaction (QCISD(T)) and Møller-Plesset perturbation theory (MP2) methods with varyingly sized basis sets (see [22] for more details) to determine single point energies of stationary points characterised at the B3LYP/6-31G*

3

level of theory. In the instance of the cyclisation reaction of 4-hydroperoxyl-but-2-yl radical forming 2-methyloxetane and a hydroxyl radical, the 0 K barrier determined in both studies differs by 13.1 kcal mol^{-1}! Further evidence of the under-prediction of reaction barriers for these reactions by the CBS-QB3 method is observed in the recent study of Zhang *et al.* on the oxidation of *n*-hexane [19]. It was found that without significant modifications to the rate rules proposed by Villano *et al.* [7] for this reaction class, model-predicted cyclic ether concentrations were too high when compared to those measured in a jet-stirred reactor. Although the determination of accurate thermochemistry is not the focus of this study, it is noteworthy that the CBS-QB3 method has recently been shown to lack both accuracy and precision when deriving enthalpies of formation *via* the atomisation method for a range of hydrocarbon and oxygenated species [20,23,24].

This study aims to provide high-fidelity rate coefficients for the reactions of interest through utilisation of high-level quantum chemical methods. A comprehensive set of reactions is chosen in order to allow application of the values derived in this work to similar reactions occurring in larger molecules, for which the use of computational methods such as those employed here is currently impractical.

2. Computational methods

2.1. Rate coefficient determination

All calculations have been performed using Gaussian 09 [16]. Geometries of minima and transition state (TS) structures have been optimised using the M06-2X functional [25] with the 6-311++G(d,p) basis set. Harmonic frequency analyses were employed at the same level of theory to verify the nature of the stationary points, with a single imaginary frequency indicative of a first-order saddle point on the potential energy surface (PES), corresponding to a TS structure. All frequencies were scaled by 0.98, with zero point vibrational energies (ZPVEs) scaled by 0.97, as recommended for the M06-2X functional by Zhao and Truhlar [25]. Intrinsic reaction coordinate (IRC) calculations [26]

4

were carried out with M06-2X/6-311++G(d,p) on each TS to ensure it was connected to the desired reactants and products. Single point energy (SPE) calculations have been carried out for all $C_2H_5O_2$ and $C_3H_7O_2$ reactants and TSs using the coupled cluster (CCSD(T)) method and employing relatively large basis sets (cc-pVTZ and cc-pVQZ [27]). The resulting energies were extrapolated to the complete basis set (CBS) limit using the following formula [28,29]:

$$E_{CCSD(T)/CBS} = E_{CCSD(T)/QZ} + (E_{CCSD(T)/QZ} - E_{CCSD(T)/TZ})\, 4^4 / 5^4 - 4^4 \qquad (1)$$

where TZ and QZ are abbreviations for cc-pVTZ and cc-pVQZ, respectively. For the $C_4H_9O_2$ and $C_5H_{11}O_2$ species, the CCSD(T)/cc-pVQZ calculations were computationally prohibitive. For these species, the CBS energies were estimated based on extrapolations of CCSD(T)/cc-pVDZ and CCSD(T)/cc-pVTZ energies. The MP2 method was then used to correct for the difference in cc-pVDTZ and cc-pVTQZ extrapolation energies. Here, cc-pVDTZ and cc-pVTQZ represent CBS extrapolations based on cc-pVDZ and cc-pVTZ, and cc-pVTZ and cc-pVQZ energies, respectively. The final energies were calculated using the following formula:

$$E_{CCSD(T)/CBS} = E_{CCSD(T)/TZ} + (E_{CCSD(T)/TZ} - E_{CCSD(T)/DZ})\, 3^4 / 4^4 - 3^4 + E_{MP2/QZ} + (E_{MP2/QZ} - E_{MP2/TZ})\, 4^4 /$$
$$5^4 - 4^4 - E_{MP2/TZ} - (E_{MP2/TZ} - E_{MP2/DZ})\, 3^4 / 4^4 - 3^4 \qquad (2)$$

Similar approaches have previously been used to approximate "higher-level" SPEs [30–32]. The validity of the approximation is investigated in this study by comparing the CCSD(T)/cc-pVTQZ energies of the $C_2H_5O_2$ and $C_3H_7O_2$ species with those determined using Eq. (2). This is further discussed in Section 3.1.

The T1 diagnostic [33] for all reactant species is ≤0.013, indicating that the use of single-reference methods to describe the wave function is appropriate. T1 values for the TSs range from 0.031 to 0.040. While T1 values greater than 0.03 (for radicals) may be cause for concern [34], none of the TSs have an unusually high value, with only six of the forty three complexes having a value greater

than 0.035. Nevertheless, if lower uncertainties are required for the TS energies, multi-reference calculations are recommended.

Relaxed PES scans were carried out for internal rotations corresponding to low frequency torsional modes in 10 degree increments as a function of dihedral angle with M06-2X/6-311++G(d,p). Rotational constants were computed as a function of dihedral angle using the Lamm module of the MultiWell program suite [35]. The resulting values were fitted to truncated Fourier series, and used as input for 1-D hindered internal rotation approximations.

The Thermo application of MultiWell was used to compute high-pressure limit rate coefficients as a function of temperature (298.15–2000 K) from canonical transition state theory [36]. Quantum mechanical tunnelling has been accounted for *via* inclusion of 1-D tunnelling through an unsymmetrical Eckart energy barrier [37]. The height of reaction barrier in the reverse direction is required to account for tunnelling, yet we have not refined the SPEs of the reaction products past that determined from the IRC analysis using M06-2X/6-311++G(d,p). This is due to the insensitivity of the computed rate coefficients for reaction in the forward direction to the height of the barrier in the reverse. Tests show that at 800 K a 10 kcal mol^{-1} variation in the reverse barrier results in a difference of ~1% in rate coefficient in the forward direction. Therefore, we find it unnecessary to determine the SPEs of the products to a higher accuracy. The resulting rate coefficients were fitted to the following modified Arrhenius expression:

$$k = A \left(T/T_{\text{ref}}\right)^{n} \exp(-E/RT) \qquad (3)$$

where A is the A-factor, T is the temperature in units of Kelvin, $T_{\text{ref}} = 1$ K, n is the temperature exponent, and E is related to the activation energy (by $E_a = E + nRT$). This modified Arrhenius form was adequate to represent the numerical data, with a maximum deviation of 14% between computed and fitted rate coefficients. These expressions of the rate coefficients are listed in Table 1, Section 3.2.

6

2.2. Uncertainty

Zádor *et al*. [38] highlight an example of uncertainties in reaction barrier determinations for a benchmark set of twenty H-atom abstraction reactions compiled by Lynch *et al*. [39]. Senosiain *et al*. [40] tested a variety of methods against seventeen of these reactions in an attempt to quantify uncertainty in reaction barrier determination for each method. Geometries were optimised using either B3LYP [41] or MP2 [42] methods with the 6-311++G(d,p) basis set. SPE calculations were carried out using B3LYP, MP2, QCISD(T), and CCSD(T) methods with augmented and non-augmented cc-pVTZ and cc-pVQZ basis sets extrapolated to the CBS limit. Absolute error values are lowest for the QCISD(T) and CCSD(T) methods, with >50% of the calculated barriers within 1 kcal mol^{-1} of the benchmark values. The absolute errors for these cases appear to be largely independent of the method used for geometry optimisation. The methods used here are quite similar to those used by Senosiain *et al*., so their results may be useful for estimation of uncertainties in the barrier heights presented here, although the are different from those compiled by Lynch *et al*. [39]. If it is assumed that the uncertainties in barrier heights calculated in this study are normally distributed, with 50% of the probability density function within 1 kcal mol^{-1} of the calculated value, we arrive at a 1σ uncertainty of 1.5 kcal mol^{-1}, which equates to a factor of ~2.6 uncertainty in rate constant at 800 K.

Estimating uncertainties in frequency factors is more difficult. The assumption that individual contributions of hindered rotors are separable is likely to be adequate for the reactions of interest in this study due to the lack of long-range interactions within the molecules. Interactions such as hydrogen bonding tend to be more prevalent in molecules or complexes with multiple oxygenated moieties, and leads to coupling of the internal rotors. This coupling, and the adequate treatment of rotors when it occurs, has been discussed previously by Sharma *et al*. [1], and suitable methods were applied to reactions of hydroperoxyl-alkyl-peroxyl radicals. Although the coupling of rotors is likely to be significant in this study, neither is it likely that there is complete separability of rotors. On this basis we estimate that uncertainties in frequency factors to be approximately a factor of 2.

7

3. Results and Discussion

3.1. Validity of CBS limit extrapolation approach

Barrier heights ($E_{0\,K}$ + ZPVE) calculated using both Eq. (1) and Eq. (2) for the reactions of $C_2H_5O_2$ and $C_3H_7O_2$ species are compared, and are tabulated in the Supplementary Material, Table S1. It is found that the barriers determined using coupled cluster and MP2 methods (denoted CC/MP2 hereafter) are consistently higher than those calculated using the coupled cluster (CC) method alone. The difference in values is quite consistent, with Eq. 2 giving barriers which are higher by an average of 0.46 kcal mol^{-1}, with a 2σ dispersion of 0.09 kcal mol^{-1}. The comparison set is small, but with such a consistent offset it seems reasonable to lower the barriers calculated using Eq. (2) for all of the reactions of $C_4H_9O_2$ and $C_5H_{11}O_2$ species by 0.46 kcal mol^{-1} from their CC/MP2 values. This amount is within the uncertainty of the calculated barrier heights, but the aim is that this offset will result in a more consistent set of values overall.

Commented [N1]: Not sure this is convincing.

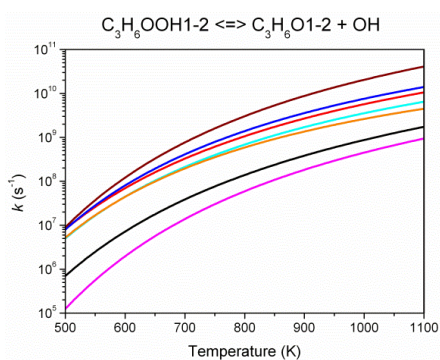### 3.2. Comparisons with the literature

Computed rate coefficients are presented in Table 1. Due to spatial constraints we provide comparisons of these rate coefficients with literature values, as well as a detailed glossary of all species listed in Table 1, as Supplementary Material. However, an account of the results is also given here. As discussed in Section 1, Villano *et al*. [7] note that the barrier heights for these reactions calculated by DeSain *et al*. [22] are an average of 2.4 kcal mol^{-1} higher than their own. The values calculated in this study fall between those calculated in the two studies, with barrier heights an average of 1.2 kcal mol^{-1} higher than those determined by Villano *et al*. [7]. This may provide yet more evidence that CBS-QB3 tends to under-predict barrier heights.

Table 1. Rate coefficients calculated in this study.

Reaction	A (s^{-1})	n	E (cal mol^{-1})
$\dot{C}_2H_4OOH1–2 \leftrightarrow C_2H_4O1–2 + \dot{O}H$	1.675×10^{07}	1.40	10880.
$\dot{C}_3H_6OOH1–2 \leftrightarrow C_3H_6O1–2 + \dot{O}H$	1.448×10^{07}	1.46	11850.
$\dot{C}_3H_6OOH1–3 \leftrightarrow C_3H_6O1–3 + \dot{O}H$	7.556×10^{05}	1.56	18070.
$\dot{C}_3H_6OOH2–1 \leftrightarrow C_3H_6O1–2 + \dot{O}H$	1.194×10^{08}	1.26	11630.
$\dot{C}_4H_8OOH1–2 \leftrightarrow C_4H_8O1–2 + \dot{O}H$	3.060×10^{07}	1.41	11310.
$\dot{C}_4H_8OOH1–3 \leftrightarrow C_4H_8O1–3 + \dot{O}H$	6.571×10^{04}	1.79	16150.
$\dot{C}_4H_8OOH1–4 \leftrightarrow C_4H_8O1–4 + \dot{O}H$	1.379×10^{05}	1.44	9920.
$\dot{C}_4H_8OOH2–1 \leftrightarrow C_4H_8O1–2 + \dot{O}H$	5.058×10^{08}	1.11	11030.
$\dot{C}_4H_8OOH2–3 \leftrightarrow C_4H_8O2–3anti + \dot{O}H$	8.979×10^{07}	1.22	10260.
$\dot{C}_4H_8OOH2–3 \leftrightarrow C_4H_8O2–3syn + \dot{O}H$	3.162×10^{08}	1.04	9930.
$\dot{C}_4H_8OOH2–4 \leftrightarrow C_4H_8O1–3 + \dot{O}H$	3.570×10^{06}	1.36	16760.
$\dot{C}_4H_8OOHI–I \leftrightarrow C_4H_8OI–I + \dot{O}H$	9.301×10^{05}	1.57	16670.
$\dot{C}_4H_8OOHI–T \leftrightarrow C_4H_8OI–T + \dot{O}H$	2.642×10^{07}	1.35	10270.
$\dot{C}_4H_8OOHT–I \leftrightarrow C_4H_8OI–T + \dot{O}H$	4.527×10^{08}	1.04	9930.
$\dot{C}_5H_{10}OOH1–2 \leftrightarrow C_5H_{10}O1–2 + \dot{O}H$	4.667×10^{12}	0.25	12840.
$\dot{C}_5H_{10}OOH1–3 \leftrightarrow C_5H_{10}O1–3 + \dot{O}H$	1.275×10^{05}	1.83	14460.
$\dot{C}_5H_{10}OOH1–4 \leftrightarrow C_5H_{10}O1–4 + \dot{O}H$	4.728×10^{05}	1.24	8130.
$\dot{C}_5H_{10}OOH1–5 \leftrightarrow C_5H_{10}O1–5 + \dot{O}H$	2.314×10^{04}	1.31	8550.
$\dot{C}_5H_{10}OOH2–1 \leftrightarrow C_5H_{10}O1–2 + \dot{O}H$	2.567×10^{09}	1.04	11340.
$\dot{C}_5H_{10}OOH2–3 \leftrightarrow C_5H_{10}O2–3anti + \dot{O}H$	4.663×10^{08}	1.09	9850.
$\dot{C}_5H_{10}OOH2–3 \leftrightarrow C_5H_{10}O2–3syn + \dot{O}H$	7.464×10^{08}	0.70	9270.
$\dot{C}_5H_{10}OOH2–4 \leftrightarrow C_5H_{10}O2–4anti + \dot{O}H$	3.835×10^{06}	1.26	14970.
$\dot{C}_5H_{10}OOH2–4 \leftrightarrow C_5H_{10}O2–4syn + \dot{O}H$	1.392×10^{06}	1.49	15210.
$\dot{C}_5H_{10}OOH2–5 \leftrightarrow C_5H_{10}O1–4 + \dot{O}H$	3.785×10^{05}	1.28	10220.
$\dot{C}_5H_{10}OOH3–1 \leftrightarrow C_5H_{10}O1–3 + \dot{O}H$	2.398×10^{06}	1.52	17240.
$\dot{C}_5H_{10}OOH3–2 \leftrightarrow C_5H_{10}O2–3anti + \dot{O}H$	2.814×10^{09}	0.35	9860.
$\dot{C}_5H_{10}OOH3–2 \leftrightarrow C_5H_{10}O2–3syn + \dot{O}H$	4.195×10^{09}	0.71	10050.
$\dot{C}_5H_{10}OOHA–A \leftrightarrow C_5H_{10}OA–A + \dot{O}H$	2.368×10^{05}	1.77	16610.

Commented [N2]: Should we report these to three places of decimals? 8.979 down below is pretty close to 8.98…

|			
$\dot{C}_5H_{10}OOHA–B \leftrightarrow C_5H_{10}OA–B + \dot{O}H$	2.440×10^{08}	1.22	10420.
$\dot{C}_5H_{10}OOHA–C \leftrightarrow C_5H_{10}OA–Canti + \dot{O}H$	1.158×10^{04}	1.96	16160.
$\dot{C}_5H_{10}OOHA–C \leftrightarrow C_5H_{10}OA–Csyn + \dot{O}H$	4.254×10^{04}	1.78	14740.
$\dot{C}_5H_{10}OOHA–D \leftrightarrow C_5H_{10}OA–D + \dot{O}H$	5.363×10^{05}	1.27	9350.
$\dot{C}_5H_{10}OOHB–A \leftrightarrow C_5H_{10}OA–B + \dot{O}H$	1.588×10^{09}	0.85	9590.
$\dot{C}_5H_{10}OOHB–C \leftrightarrow C_5H_{10}OB–C + \dot{O}H$	8.638×10^{08}	0.85	8780.
$\dot{C}_5H_{10}OOHB–D \leftrightarrow C_5H_{10}OB–D + \dot{O}H$	1.205×10^{07}	1.22	16390.
$\dot{C}_5H_{10}OOHC–A \leftrightarrow C_5H_{10}OA–Canti + \dot{O}H$	3.786×10^{03}	2.69	14900.
$\dot{C}_5H_{10}OOHC–A \leftrightarrow C_5H_{10}OA–Csyn + \dot{O}H$	2.207×10^{05}	1.67	16240.
$\dot{C}_5H_{10}OOHC–B \leftrightarrow C_5H_{10}OB–C + \dot{O}H$	1.191×10^{10}	0.77	9420.
$\dot{C}_5H_{10}OOHC–D \leftrightarrow C_5H_{10}OC–D + \dot{O}H$	1.230×10^{09}	1.01	10180.
$\dot{C}_5H_{10}OOHD-A \leftrightarrow C_5H_{10}OA–D + \dot{O}H$	4.604×10^{05}	1.30	9360.
$\dot{C}_5H_{10}OOHD-B \leftrightarrow C_5H_{10}OB–D + \dot{O}H$	1.142×10^{05}	1.65	13370.
$\dot{C}_5H_{10}OOHD-C \leftrightarrow C_5H_{10}OC–D + \dot{O}H$	1.726×10^{07}	1.41	11350.
$neo\dot{C}_5H_{10}OOH \leftrightarrow neoC_5H_{10}O + \dot{O}H$	5.882×10^{06}	1.55	15990.

Figure 1. Comparison of literature values with this work for the cyclisation reaction of 3-hydroperoxyl-prop-2-yl radical forming methyloxirane and a hydroxyl radical. Black: *This work*, **Red: Villano** *et al*. **[7], Blue: Miyoshi [3], Magenta: Wijaya** *et al*. **[43], Cyan: Cord** *et al*. **[44], Wine: Chan** *et al*. **[45], Orange: Goldsmith** *et al*. **[31].**

An example comparison of literature rate coefficients is shown in Fig. 1 for the cyclisation reaction of 3-hydroperoxyl-prop-2-yl radical forming methyloxirane and a hydroxyl radical. This comparison reflects the general trend seen when comparing literature rate coefficients with those calculated in this study, in that those computed here tend towards the lower end of values which currently exist.

These lower rate coefficients may have been expected due to the findings of Zhang *et al*. [19], where some of the rate rules suggested by Villano *et al*. [7] had to be lowered by approximately a factor of 4 in the temperature region where these reactions are most important (~700–900 K) in order to improve model agreement with cyclic ether concentration profiles measured using a jet-stirred reactor. This was achieved by lowering the A-factor of the Arrhenius expressions by a factor of 2, and increasing the activation energy by 1 kcal mol^{-1}.

3.3. Implications for combustion modelling

Figure 2 shows the effects of including the rate coefficients presented here for the reactions of $C_5H_{11}O_2$ to a recently published model describing oxidation of the pentane isomers [18]. Constant volume and perfectly-stirred reactor simulations were run under some representative conditions in which chemical kinetic models describing combustion processes are often validated. *n*-Pentane is chosen as the representative fuel, and CHEMKIN-PRO [46] was used for the simulations. The closed homogeneous batch reactor, and perfectly-stirred reactor modules within CHEMKIN-PRO were used to simulate the ignition delay times and species concentration profiles, respectively. Ignition delay simulations were run under stoichiometric fuel/'air' conditions (2.56% *n*-pentane, 20.46% O_2, 76.98% N_2) at 10 and 20 atm, and from 650–1400 K. The perfectly-stirred reactor simulations were also run under stoichiometric conditions (1% *n*-pentane, 8% O_2, 91% N_2) at 1 atm, and from 500–1100 K, at a residence time of 2 s. Also plotted are data presented in [18], Fig. 2 (a), as well as jet-stirred reactor data yet to be published [47], Fig. 2 (b) and (c).

11
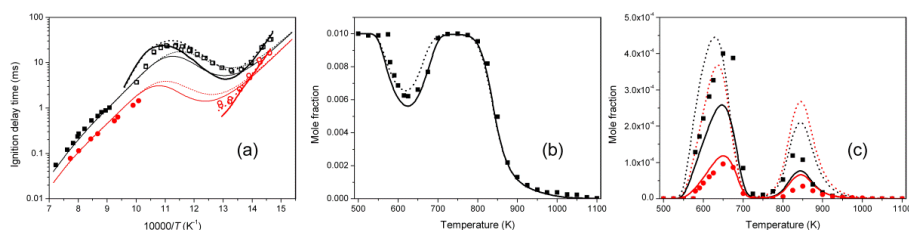
Figure 2. Model-simulated effects of rate coefficients presented in this study on *n*-pentane (a) ignition delay times at 10 (black) and 20 atm (red), and perfectly-stirred reactor profiles of (b) *n*-pentane, (c) 2-methyltetrahydrofuran (black), and 2,4-dimethyloxetane (red). Symbols represent experimental data, dashed lines represent Model A, and solid lines Model B (see Section 3.3 for details). The thicker lines in (a) represent simulations accounting for facility effects.

The simulation results of two models (Model A and Model B) are shown. Model A is that presented in [18], with the rate coefficients for C_5 cyclic ether formation reactions taken from Villano *et al*. [7]. Model B is the same, but with the rate coefficients for the same reaction class replaced with those pertaining to *n*-pentane from Table 1 in this study. It is shown that there is an increase in reactivity in the NTC region in both sets of simulations, where the title reactions are known to be important, Fig. 2 (a) and (b). This reaction class is an important radical chain propagating one, and so this effect is as expected given that the newly computed rate coefficients are lower than those from Villano *et al*. [7]. The effects seen are not big in terms of overall reactivity, but in Fig. 2 (c) the perfectly-stirred reactor simulated concentration profiles of the two major cyclic ethers formed from *n*-pentane oxidation (2-methyltetrahydrofuran and 2,4-dimethyloxetane) are shown, and a significant effect *is* seen. Two peaks are observed in both concentration profiles at approximately 650 and 850 K, and factors of ~2–4 differences are seen in the simulated profiles at these temperatures. While model-predicted mole fractions of 2-methyltetrahydrofuran have gone from slightly over-predicting the experimental data to under-predicting it, those of 2,4-dimethyloxetane have improved considerably in terms of

12

agreement with experiment. While the graphs in Fig. 2 are mainly for illustrative purposes, it is seen that the inclusion of the newly calculated rate coefficients into an existing model can bring about significant changes and overall improvement in predicting cyclic ether concentrations. Model B would require modifications in order to restore the accurate prediction of overall reactivity, but this test provides insights into the modelling implications of using the rate coefficients presented in Table 1.

4. Conclusions

This paper presents a systematic and comprehensive study of the high-pressure limit kinetics of cyclic ether formation reactions from hydroperoxyl-alkyl radicals. The rate coefficients are presented and compared with those from the literature, and we find that those presented here are generally lower than the existing values. Two different approaches are compared for the determination of reaction barrier heights, and we validate a method which can approximate a "higher-level" answer at a lower computational cost. The implications that these new rate coefficients may have for combustion modelling are discussed, with results that are reasonably significant in terms of mechanism predictions.

While this study presents values which are determined at a higher level of theory than other studies for this reaction class, the modelling successes achieved by using values from these previous studies cannot be understated. Several recent studies emanating from this research group and collaborators have proven just how useful systematic studies of important reaction classes can be, even if the accuracy of those values are not state-of-the-art. It is likely that these successes were possible due to most of the rate coefficients for important reaction classes within low-temperature oxidation schemes being calculated at the same level of theory (CBS-QB3). While the absolute accuracies of the values are probably less than desirable, it may be the case that the relative values are more preferable, resulting in favourable model predictions.

A more accurate determination of uncertainties in rate coefficients derived using different theoretical methods would be extremely useful for chemical kinetic modellers. A benchmarking study of different model chemistries, for instance, would go a long way in this regard. However, obtaining suitable experimental data is likely difficult or currently impossible, so any such studies would have to rely on comparisons with state-of-the-art theoretical calculations. Computationally less accurate (and cheaper) methods with more accurate uncertainties may prove to be the most useful.

Acknowledgements

14

References

[1] S. Sharma, S. Raman, W. H. Green, *J. Phys. Chem. A* 114 (2010) 5689–5701.

[2] F. Zhang, T. S. Dibble, *J. Phys. Chem. A* 115 (2011) 655–663.

[3] A. Miyoshi, *J. Phys. Chem. A* 115 (2011) 3301–3325.

[4] J. Zádor, S. J. Klippenstein, J. A. Miller, *J. Phys. Chem. A* 115 (2011) 10218–10225.

[5] S. M. Villano, L. K. Huynh, H. -H. Carstensen, A. M. Dean, *J. Phys. Chem. A* 115 (2011) 13425–13442.

[6] A. Miyoshi, *Int. J. Chem. Kinet.* 44 (2012) 59–74.

[7] S. M. Villano, L. K. Huynh, H. -H. Carstensen, A. M. Dean, *J. Phys. Chem. A* 116 (2012) 5068–5089.

[8] S. M. Villano, H. -H. Carstensen, A. M. Dean, *J. Phys. Chem. A* 117 (2013) 6458–6473.

[9] J. A. Montgomery, M. J. Frisch, J. W. Ochterski, G. A. Petersson, *J. Chem. Phys.* 112 (2000) 6532–6542.

[10] J. W. Ochterski, G. A. Petersson, J. A. Montgomery, *J. Chem. Phys.* 104 (1996) 2598–2619.

[11] J. A. Pople, M. Head-Gordon, D. J. Fox, K. Raghavachari, L. A. Curtiss, *J. Chem. Phys.* 90 (1989) 5622–5629.

[12] L. A. Curtiss, C. Jones, G. W. Trucks, K. Raghavachari, J. A. Pople, *J. Chem. Phys.* 93 (1990) 2537–2545.

[13] L. A. Curtiss, K. Raghavachari, G. W. Trucks, J. A. Pople, *J. Chem. Phys.* 94 (1991) 7221–7230.

[14] L. A. Curtiss, K. Raghavachari, P. C. Redfern, V. Rassolov, J. A. Pople, *J. Chem. Phys.* 109 (1998) 7764–7776.

[15] L. A. Curtiss, P. C. Redfern, K. Raghavachari, *J. Chem. Phys.* 126 (2007) 084108.

[16] M. J. Frisch, G. W. Trucks, H. B. Schlegel, G. E. Scuseria, M. A. Robb, J. R. Cheeseman, G. Scalmani, V. Barone, B. Mennucci, G. A. Petersson, H. Nakatsuji, M. Caricato, X. Li, H. P. Hratchian, A. F. Izmaylov, J. Bloino, G. Zheng, J. L. Sonnenberg, M. Hada, M. Ehara, K. Toyota, R. Fukuda, J. Hasegawa, M. Ishida, T. Nakajima, Y. Honda, O. Kitao, H. Nakai, T. Vreven, J. A. Montgomery, J. E. Peralta, F. Ogliaro, M. Bearpark, J. J. Heyd, E. Brothers, K. N. Kudin, V. N. Staroverov, R. Kobayashi, J. Normand, K. Raghavachari, A. Rendell, J. C. Burant, S. S. Iyengar, J. Tomasi, M. Cossi, N. Rega, J. M. Millam, M. Klene, J. E. Knox, J. B. Cross, V. Bakken, C. Adamo, J. Jaramillo, R. Gomperts, R. E. Stratmann, O. Yazyev, A. J. Austin, R. Cammi, C. Pomelli, J. W. Ochterski, R. L. Martin, K. Morokuma, V. G. Zakrzewski, G. A. Voth, P. Salvador, J. J. Dannenberg, S. Dapprich, A. D. Daniels, Ö. Farkas, J. B. Foresman, J. V. Ortiz, J. Cioslowski, D. J. Fox, Gaussian 09, revision D.01; Gaussian, Inc., Wallingford, CT, 2009.

[17] J. Bugler, K. P. Somers, E. J. Silke, H. J. Curran, *J. Phys. Chem. A* 119 (2015) 7510–7527.

[18] J. Bugler, B. Marks, O. Mathieu, R. Archuleta, A. Camou, C. Grégoire, K. A. Heufer, E. L. Petersen, H. J. Curran, *Combust. Flame* (2015) in press, doi:10.1016/j.combustflame.2015.09.014

[19] K. Zhang, C. Banyon, C. Togbé, P. Dagaut, J. Bugler, H. J. Curran, *Combust. Flame* 162 (2015) 4194–4207.

[20] J. M. Simmie, K. P. Somers, *J. Phys. Chem. A* 119 (2015) 7235–7246.

[21] J. Aguilera-Iparraguirre, H. J. Curran, W. Klopper, J. M. Simmie, *J. Phys. Chem. A* 112 (2008) 7047–7054.

[22] J. D. DeSain, C. A. Taatjes, J. A. Miller, S. J. Klippenstein, D. K. Hahn, *Faraday Discuss.* 119 (2001) 101−120.

[23] K. P. Somers, J. M. Simmie, *J. Phys. Chem. A* 119 (2015) 8922–8933.

[24] J. M. Simmie, *J. Phys. Chem. A* 119 (2015) 10511–10526.

[25] Y. Zhao, D. G. Truhlar, *Theor. Chem. Account.* 120 (2008) 215–241.

[26] H. P. Hratchian, H. B. Schlegel, *J. Chem. Theory Comput.* 1 (2005) 61−69.

[27] T. H. Dunning, *J. Chem. Phys.* 90 (1989) 1007−1023.

[28] J. M. L. Martin, *Chem. Phys. Lett.* 259 (1996) 669−678.

[29] D. Feller, D. A. Dixon, *J. Chem. Phys.* 115 (2001) 3484−3496.

[30] J. A. Miller, S. J. Klippenstein, *J. Phys. Chem. A* 107 (2003) 7783–7799.

[31] C. F. Goldsmith, W. H. Green, S. J. Klippenstein, *J. Phys. Chem. A* 116 (2012) 3325–3346.

[32] C. F. Goldsmith, G. R. Magoon, W. H. Green, *J. Phys. Chem. A* 116 (2012) 9033–9057.

[33] T. J. Lee, P. R. Taylor, *Int. J. Quantum Chem.: Quantum Chemistry Symposium* 23 (1989) 199–207.

[34] S. J. Klippenstein, L. B. Harding, *Proc. Combust. Inst.* 32 (2009) 149–155.

[35] MultiWell-2014.1 Software, 2014, designed and maintained by J. R. Barker with contributors N. F. Ortiz, J. M. Preses, L. L. Lohr, A. Maranzana, P. J. Stimac, T. L. Nguyen, and T. J. D. Kumar, University of Michigan, Ann Arbor, MI, http://aoss.engin.umich.edu/multiwell/.

[36] H. Eyring, *J. Chem. Phys.* 3 (1935) 107−115.

[37] C. Eckart, *Phys. Rev.* 35 (1930) 1303–1309.

17

[38] J. Zádor, C. A. Taatjes, R. X. Fernandes, *Prog. Energy Combust. Sci.* 37 (2011) 371–421.

[39] B. J. Lynch, P. L. Fast, M. Harris, D. G. Truhlar, *J. Phys. Chem. A* 104 (2000) 4811–4815.

[40] J. P. Senosiain, S. J. Klippenstien, J. A. Miller, unpublished data.

[41] C. Lee, W. Yang, R. G. Parr, *Phys. Rev. B* 37 (1988) 785–789.

[42] C. Møller, M. S. Plesset, *Phys. Rev.* 46 (1934) 618–622.

[43] C. D. Wijaya, R. Sumathi, W. H. Green, *J. Phys. Chem. A* 107 (2003) 4908–4920.

[44] M. Cord, B. Sirjean, R. Fournet, A. Tomlin, M. Ruiz-Lopez, F. Battin-Leclerc, *J. Phys. Chem. A* 116 (2012) 6142–6158.

[45] W. -T. Chan, H. O. Pritchard, I. P. Hamilton, *Phys. Chem. Chem. Phys.* 16 (1999) 3715–3719.

[46] CHEMKIN-PRO 15101; Reaction Design: San Diego, 2010.

[47] ...